The velocity-dissipation probability density function model for turbulent flows

S. B. Pope and Y. L. Chen[a)]
Sibley School of Mechanical and Aerospace Engineering, Cornell University, Ithaca, New York 14853

(Received 1 December 1989; accepted 25 April 1990)

In probability density function (pdf) methods, statistics of inhomogeneous turbulent flow fields are calculated by solving a modeled transport equation for a one-point joint probability density function. The method based on the joint pdf of velocity and fluid compositions is particularly successful since the most important processes—convection and reaction—do not have to be modeled. However, this joint pdf contains no length-scale or time-scale information that can be used in the modeling of other processes. This deficiency can be remedied by considering the joint pdf of velocity, dissipation, and composition. In this paper, by reference to the known properties of homogeneous turbulence, a modeled equation for the joint pdf of velocity and dissipation is developed. This is achieved by constructing stochastic models for the velocity and dissipation following a fluid particle.

I. INTRODUCTION

In engineering industry and elsewhere, there is an increasing use of computational methods to calculate complex turbulent flow fields and the mixing and chemical reaction that may occur within them.[1,2] Most of these computations depend upon the k-ϵ turbulence model,[3,4] while a few are based on second-order closures.[5–9] For some flows, these turbulence models provide an adequate description of the turbulent processes. But for many others, a more complete and accurate description of the turbulence is necessary. Here we present a new turbulence model designed to meet this need.

For good reason, turbulence models—e.g., mixing-length, k-ϵ, Reynolds-stress—are named after the dependent variables chosen to represent the turbulence. This choice—rather than the details of the subsequent modeling—is the principal determinant of the model's success. Ideally, the chosen representation should be sufficiently comprehensive so that (i) the dominant physical processes are treated exactly (without modeling), and (ii) there is sufficient information available to construct realistic models of the remaining processes. On the other hand, the chosen representation should be sufficiently compact so that (iii) the solution of the resulting model equations is computationally tractable.

To date, this last criterion has eliminated multipoint or spectral closures from consideration: they have not proved computationally tractable for inhomogeneous flows.

The most comprehensive one-point closure, and consequently that which fares best according to criterion (i), is based on the (one-point) joint probability density function (pdf) of the velocities and compositions.[10–13] Convection and reaction are treated exactly (without modeling), as are the mean pressure gradient and body forces. Only the effects of the fluctuating pressure gradient and molecular diffusion have to be modeled: neither of these processes affects the mean velocities or compositions directly.

Because it treats convection exactly, the velocity-composition pdf method accurately represents transport processes in some flows for which other models fail. We cite two examples. In the dispersion of heat from a line source in grid turbulence,[14–16] models that incorporate gradient diffusion (at any level) are inaccurate and qualitatively incorrect near the source[17] (where the length scale of the thermal field is very small compared to the integral scale of the turbulence). But the pdf method accurately describes the dispersion, both near the source and downstream.[18] In statistically plane premixed turbulent flames, the mean pressure field affects the fluctuating velocity field in such a way as to produce counter-gradient transport.[19] This is accurately represented in pdf methods[20]—since both the mean pressure gradient and convection are treated without approximation—but clearly a model that incorporates gradient-diffusion transport is qualitatively incorrect for this flow.

Considering the large amount of information embodied in the velocity-composition joint pdf, it is perhaps surprising that this approach is computationally tractable. But Monte Carlo methods have been developed,[21,11,22] demonstrated, and used for a variety of flows. These include: turbulent jet diffusion flames;[23,24] two-dimensional recirculating flows;[25] and, the flow within spark-ignition engine cylinders.[26,27]

In a crucial respect, the velocity-composition joint pdf approach fails according to criterion (ii): The joint pdf contains no information about turbulent length scales or time scales. Consequently, additional assumptions or model equations are required. For several free shear flows, the assumption has been made[13,21–24] that the turbulent time scale $\tau \equiv k/\langle\epsilon\rangle$ is uniform across the flow. (Here, k is the turbulent kinetic energy and $\langle\epsilon\rangle$ is the mean dissipation rate.) For other flows, the standard model equation[3,4] for $\langle\epsilon\rangle$ has been solved,[26,27] or, similarly, a model equation[28] for $\langle\omega\rangle \equiv 1/\tau = \langle\epsilon\rangle/k$.

The model developed here is based on the one-point joint pdf of velocity and the instantaneous dissipation rate ϵ. This joint pdf contains length-scale and time-scale information (e.g., $k^{3/2}/\langle\epsilon\rangle$ and $k/\langle\epsilon\rangle$), and hence remedies the incompleteness of the velocity-composition joint pdf approach. But more than this: The inclusion of ϵ within the pdf approach opens the way to more realistic modeling. Large

[a)] Permanent address: University of Science and Technology of China, Hefei, Anhui, People's Republic of China.

 0899-8213/90/081437-13$02.00

fluctuations in the dissipation rate (i.e., internal intermittency) are accounted for; and, in inhomogeneous flows, fuller account can be taken of the different behavior of turbulent fluid, depending on its origin and history.

Previously, a model based on the joint pdf of velocity and a *conditional mean dissipation* has been developed and applied[29] to the shear-free mixing layer between two regions of turbulence with different scales and intensities.[30] The success of the model in this application illustrates one of the attributes (mentioned above) of this type of model: namely, the ability to account for effects of history on fluid-particle behavior. The model developed here is significantly different in that a more sophisticated model for the *instantaneous dissipation* is proposed.

As in previous pdf studies,[11-13] we take a Lagrangian view in performing the modeling. Specifically, we construct stochastic models [$\mathbf{U}^*(t)$ and $\epsilon^*(t)$] for the velocity and dissipation following a fluid particle. By definition, the position of the fluid particle $\mathbf{x}^*(t)$ moves with velocity $\mathbf{U}^*(t)$; while (by assumption) $\mathbf{U}^*(t)$ and $\epsilon^*(t)$ evolve according to coupled diffusion processes.[11,31] Thus $\mathbf{x}^*(t)$, $\mathbf{U}^*(t)$, and $\epsilon^*(t)$ jointly form a Markov process that is continuous in time. These stochastic models provide a closure for the one-point Eulerian velocity-dissipation joint pdf equation, and also for the multitime Lagrangian joint pdf equation.

In this paper the stochastic models for $\epsilon^*(t)$ (Sec. II) and $\mathbf{U}^*(t)$ (Sec. III) are developed by requiring that they have the correct behavior in homogeneous turbulence. Then, in a subsequent paper,[32] the model is extended and applied to a variety of inhomogeneous flows. (For simplicity we do not consider compositions: The extension to the joint pdf of velocity, dissipation, and compositions is straightforward.[2])

The model equations contain a number of coefficients. For definiteness, the values ascribed to these coefficients are stated as they occur; but the justification for these specifications is postponed to Sec. V.

II. STOCHASTIC MODEL FOR DISSIPATION

A. Definitions

We consider homogeneous turbulence in a Newtonian fluid of constant density ρ and kinematic viscosity ν. At position $\mathbf{x}$ and time t, the Eulerian velocity is $\mathbf{U}(\mathbf{x},t)$, with mean $\langle \mathbf{U}(\mathbf{x},t) \rangle$ and fluctuation $\mathbf{u}(\mathbf{x},t)$:

$$\mathbf{U}(\mathbf{x},t) = \langle \mathbf{U}(\mathbf{x},t) \rangle + \mathbf{u}(\mathbf{x},t). \tag{1}$$

The mean velocity gradients $\partial \langle U_i \rangle / \partial x_j$ may vary with time, but are spatially uniform.

Rather than the true dissipation rate

$$\epsilon_T(\mathbf{x},t) \equiv \frac{1}{2} \nu \left(\frac{\partial u_i}{\partial x_j} + \frac{\partial u_j}{\partial x_i} \right) \left(\frac{\partial u_i}{\partial x_j} + \frac{\partial u_j}{\partial x_i} \right), \tag{2}$$

we consider the pseudodissipation defined by

$$\epsilon(\mathbf{x},t) \equiv \nu \frac{\partial u_i}{\partial x_j} \frac{\partial u_i}{\partial x_j}. \tag{3}$$

The reason for this choice is that in two respects (described below) direct numerical simulations (DNS) of isotropic turbulence[33] show that the statistical properties of ϵ are more favorable than those of ϵ_T.

The true and pseudodissipation are related by

$$\epsilon = \epsilon_T - \nu \frac{\partial^2 u_i u_j}{\partial x_i \partial x_j}. \tag{4}$$

Consequently, $\langle \epsilon \rangle$ and $\langle \epsilon_T \rangle$ differ only by the factor $\nu(\partial^2 / \partial x_i \partial x_j) \langle u_i u_j \rangle$, which is zero in homogeneous turbulence, and in general varies inversely with Reynolds number. But in spite of the negligible difference in the means, there are significant differences in other statistics.[33]

Henceforth, we refer to the pseudodissipation ϵ simply as dissipation.

It is found that the model developed here is significantly simplified if ϵ is reexpressed as the *relaxation rate* ω defined by

$$\omega(\mathbf{x},t) \equiv \epsilon(\mathbf{x},t)/k(t). \tag{5}$$

Note that ω is a mixed variable, in the sense that $\epsilon(\mathbf{x},t)$ is random whereas $k(t)$ is not. This variable—or at least its mean $\langle \omega \rangle$—has been used in several previous turbulence models.[28,34,35]

It is also convenient to define $\chi(\mathbf{x},t)$ as the logarithm of the normalized dissipation:

$$\chi(\mathbf{x},t) \equiv \ln[\epsilon(\mathbf{x},t)/\langle \epsilon(t) \rangle] = \ln[\omega(\mathbf{x},t)/\langle \omega(t) \rangle]. \tag{6}$$

The position, velocity, and dissipation of a fluid particle are denoted by $\mathbf{x}^+(t)$, $\mathbf{U}^+(t)$, and $\epsilon^+(t)$, and similarly for any other property. These Lagrangian variables are related to the Eulerian fields by, for example,

$$\omega^+(t) = \omega(x^+[t],t). \tag{7}$$

B. Statistical properties of dissipation

In the next subsection it is proposed to model $\chi^+(t)$ as an Uhlenbeck–Ornstein (UO) process[31] $\chi^*(t)$. The two principal characteristics of a UO process are that the one-time pdf is Gaussian, and that the autocorrelation is exponential. The purpose of this subsection is to show that—to a reasonable approximation—$\chi^+(t)$ does indeed share these characteristics.

In the celebrated papers of Kolmogorov[36] and Obukhov,[37] it is hypothesized that (at high Reynolds number) ϵ_T is lognormally distributed. Since then the hypothesis has been examined many times, usually with appeals to experimental data on the distribution of $(\partial u_1/\partial x_1)^2$ (see, e.g., Monin and Yaglom[38]).

More direct evidence—although restricted to moderate Reynolds numbers— comes from DNS of isotropic turbulence. Yeung and Pope[33] performed simulations up to a Taylor-scale Reynolds number R_λ of 93 and examined in detail the statistics of ϵ and ϵ_T. The relevant statistics are summarized in Table I. It may be seen that the skewness (μ_3), flatness (μ_4), and superskewness (μ_6) of $\chi = \ln(\epsilon/\langle \epsilon \rangle)$ are very close to the Gaussian values of 0, 3, and 15. On the other hand, the same moments ($\mu_3^T, \mu_4^T, \mu_6^T$) based on the true dissipation are significantly different from Gaussian. We conclude: first, that ϵ is very close to lognormal; and, second, that other related quantities [e.g., ϵ_T and $(\partial u_1/\partial x_1)^2$] may have significantly different statistics.

Figure 1 shows the autocorrelation of χ^+, $\rho_\chi(s)$, compared to the exponential e^{-s/T_χ}, where T_χ is the integral

TABLE I. Statistics of ϵ and ϵ_T from direct numerical simulations of isotropic turbulence (Ref. 33).[a]

R_λ	μ_3	μ_3^T	μ_4	μ_4^T	μ_6	μ_6^T	σ^2	T_χ/T_u
38	−0.04	−0.24	3.04	3.22	15.9	20.0	0.71	0.96
63	0.01	−0.19	3.00	3.15	15.1	18.5	0.83	0.92
93	0.00	−0.21	3.00	3.14	15.5	18.1	0.91	0.91

[a] μ_m and μ_m^T are the mth central moments of the standardized pdf 's of $\ln\epsilon$ and $\ln\epsilon_T$. σ^2 is the variance of $\ln\epsilon$. T_χ and T_u are the Lagrangian integral time scales of χ and U_1.

time scale of χ^+. At small times there is a qualitative difference between the curves. Since $\chi^+(t)$ is a differentiable process, its autocorrelation has zero slope at the origin. On the other hand, the UO process $\chi^*(t)$ is not differentiable (although it is continuous) and consequently its autocorrelation has a negative slope. But, apart from these differences at small times, the exponential provides a reasonable approximation to $\rho_\chi(s)$.

C. Stochastic model for ϵ^+

We model $\chi^+(t) = \ln(\epsilon^+/\langle\epsilon\rangle)$ by the Uhlenbeck–Ornstein process $\chi^*(t)$ with variance σ^2 and integral time scale T_χ. This is a stationary Markov process, with $\chi^*(t)$ being continuous in time, although not differentiable. The stochastic differential equation for $\chi^*(t)$ can be written

$$d\chi^* \equiv \chi^*(t+dt) - \chi^*(t) = -(\chi^* - \langle\chi^*\rangle)\frac{dt}{T_\chi} + \left(\frac{2\sigma^2}{T_\chi}\right)^{1/2} dW, \tag{8}$$

where W is a Wiener process.[11,31] (The increment dW is a Gaussian random variable with zero mean and variance dt.) Since χ^* is Gaussian and normalized so that $\langle\exp(\chi^*)\rangle$ is unity, it is readily shown (see Appendix A, for example) that its mean is

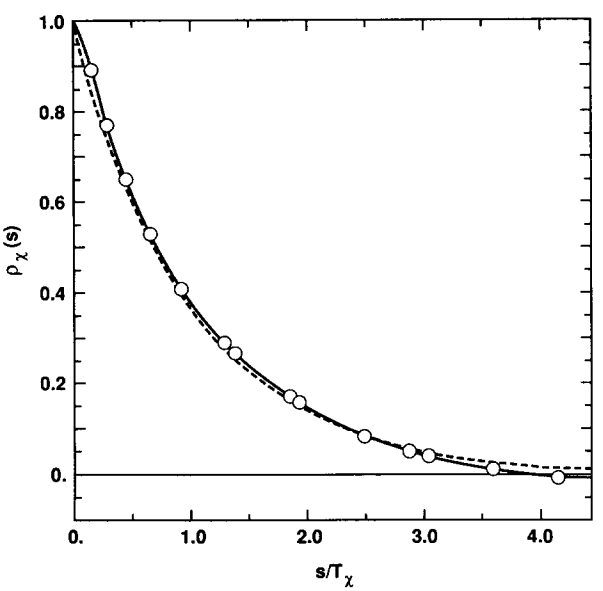

FIG. 1. Autocorrelation function of $\chi^+ \equiv \ln(\epsilon^+/\langle\epsilon\rangle)$. Solid line, from direct numerical simulations;[33] dashed line, $\exp(-s/T_\chi)$.

$$\langle\chi^*\rangle = -\tfrac{1}{2}\sigma^2. \tag{9}$$

And defining the constant C_χ by

$$T_\chi^{-1} = C_\chi\langle\omega\rangle, \tag{10}$$

we can rewrite Eq. (8) as

$$d\chi^* = -C_\chi\langle\omega\rangle(\chi^* + \tfrac{1}{2}\sigma^2)dt + (2C_\chi\langle\omega\rangle\sigma^2)^{1/2}\,dW. \tag{11}$$

For the reasons given in Sec. V, σ^2 and C_χ are ascribed the values 1.0 and 1.6, respectively.

The corresponding equation for $\epsilon^* = \langle\epsilon\rangle\exp(\chi^*)$ is obtained by use of the Ito transformation:[31]

$$d\epsilon^* = \frac{\epsilon^*}{\langle\epsilon\rangle}\frac{d\langle\epsilon\rangle}{dt}dt + \epsilon^* d\chi^* + \epsilon^*\sigma^2\frac{dt}{T_\chi}. \tag{12}$$

In order to leave the first term in a general form, we define the normalized decay rate of ϵ, S_ϵ, by

$$\frac{d\langle\epsilon\rangle}{dt} = -S_\epsilon\langle\omega\rangle\langle\epsilon\rangle. \tag{13}$$

According to the standard model equation for $\langle\epsilon\rangle$, S_ϵ is given by[3]

$$S_\epsilon = C_{\epsilon 2} - C_{\epsilon 1}P/\langle\epsilon\rangle, \tag{14}$$

where P is the rate of production of turbulent kinetic energy, and $C_{\epsilon 1}$ and $C_{\epsilon 2}$ are model constants, generally ascribed the values 1.45 and 1.90, respectively. Thus from Eqs. (11)–(13) we obtain

$$d\epsilon^* = -\epsilon^*\langle\omega\rangle dt\{S_\epsilon + C_\chi[\ln(\epsilon^*/\langle\epsilon\rangle) - \tfrac{1}{2}\sigma^2]\} + \epsilon^*(2C_\chi\langle\omega\rangle\sigma^2)^{1/2}\,dW. \tag{15}$$

The corresponding equation for $\omega^* = \epsilon^*/k$ differs only in the mean decay rate:

$$d\omega^* = -\omega^*\langle\omega\rangle dt\{S_\omega + C_\chi[\ln(\omega^*/\langle\omega\rangle) - \tfrac{1}{2}\sigma^2]\} + \omega^*(2C_\chi\langle\omega\rangle\sigma^2)^{1/2}\,dW, \tag{16}$$

where S_ω is defined by

$$\frac{d\langle\omega\rangle}{dt} = -S_\omega\langle\omega\rangle^2. \tag{17}$$

In homogeneous turbulence we have

$$\frac{dk}{dt} = P - \langle\epsilon\rangle, \tag{18}$$

and hence

$$S_\omega = S_\epsilon + P/\langle\epsilon\rangle - 1. \tag{19}$$

Or, in terms of the standard model [Eq. (14)]

$$S_\omega = (C_{\epsilon 2} - 1) - (C_{\epsilon 1} - 1)P/\langle\epsilon\rangle. \tag{20}$$

III. STOCHASTIC MODEL FOR VELOCITY

We develop here a stochastic model $\mathbf{U}^*(t)$ for the velocity following a fluid particle $\mathbf{U}^+(t)$. The starting point is the generalized Langevin model (GLM) developed by Haworth and Pope,[12,13] which is described in Sec. III A. As far as the evolution of the one-point joint pdf of velocity is concerned, this model is completely satisfactory for homogeneous turbulence: The pdf is joint normal (consistent with experimental observations[39]) and the evolution of the Reynolds stresses is accurately described. Furthermore, it has been

demonstrated[13] that the model performs well in application to free shear flows.

According to the Langevin model, for small time intervals s, the Lagrangian velocity increment

$$\Delta_s \mathbf{U}^*(t) \equiv \mathbf{U}^*(t+s) - \mathbf{U}^*(t), \tag{21}$$

is a Gaussian random variable with variance proportional to $s\langle\epsilon\rangle$. In Sec. III B evidence is presented to show that it is more accurate to model the (conditional) variance of $\Delta_s \mathbf{U}^*$ (for small s) as being proportional to $s\epsilon^*$ (rather than $s\langle\epsilon\rangle$)—thus taking account of internal intermittency. Accordingly, the generalized Langevin model for $\mathbf{U}^*(t)$ is refined to account for internal intermittency, and yet to yield the same pdf evolution (in homogeneous turbulence) as the generalized Langevin model.

A. Generalized Langevin model

The generalized Langevin model[11-13] is

$$dU_i^* = -\frac{1}{\rho}\frac{\partial\langle p\rangle}{\partial x_i}dt + G_{ij}(U_j^* - \langle U_j\rangle)dt + (C_0\langle\epsilon\rangle)^{1/2}\,dW_i, \tag{22}$$

where $\langle p\rangle$ is the mean pressure G_{ij} is a second-order tensor discussed below, C_0 is a constant ascribed the value $C_0 = 2.1$, and $\mathbf{W}(t)$ is an isotropic Wiener process with the properties

$$\langle d\mathbf{W}\rangle = 0,\ \langle dW_i\, dW_j\rangle = dt\,\delta_{ij}. \tag{23}$$

($\mathbf{W}$ is independent of the Wiener process W in the equation for ϵ^*.)

In the GLM, the tensor $G_{ij}(\mathbf{x},t)$ is a function of the local values of $\langle\omega\rangle$, $\partial\langle U_i\rangle/\partial x_j$ and the Reynolds stresses $\langle u_i u_j\rangle$. The specific form of G_{ij} is deduced by requiring that the evolution of the Reynolds stresses in homogeneous turbulence be in accord with experiments.[12] We also consider the simplified Langevin model (SLM), in which G_{ij} takes its simplest possible form. To this end we write

$$G_{ij} = -(\tfrac{1}{2} + \tfrac{3}{4}C_0)\langle\omega\rangle\delta_{ij} + G_{ij}^a, \tag{24}$$

where G_{ij}^a is zero for the SLM, and for the GLM it is defined (in terms of G_{ij}) by this equation. In isotropic turbulence without mean velocity gradients, G_{ij}^a is zero—even in the GLM. In addition, G_{ij}^a is constrained so that

$$G_{ij}^a\langle u_i u_j\rangle = 0 \tag{25}$$

[see Eq. (25) of Ref. 12].

For the case of homogeneous turbulence under consideration, it is preferable to examine the stochastic differential equation for $\mathbf{u}^*(t)$:

$$\mathbf{u}^*(t) \equiv \mathbf{U}^*(t) - \langle\mathbf{U}(\mathbf{x}^*[t],t)\rangle, \tag{26}$$

which is the excess of the Lagrangian velocity over the local Eulerian mean. In homogeneous turbulence, the one-time statistics of $\mathbf{u}^*(t)$ are identical to those of the Eulerian fluctuation $\mathbf{u}(t)$.

Corresponding to the GLM [Eq. (22)], the stochastic equation for $\mathbf{u}^*$ is

$$du_i^* = K_{ij}u_j^*\,dt + (C_0\langle\epsilon\rangle)^{1/2}\,dW_i, \tag{27}$$

where

$$K_{ij} \equiv G_{ij} - \frac{\partial\langle U_i\rangle}{\partial x_j} = -\left(\frac{1}{2} + \frac{3}{4}C_0\right)\langle\omega\rangle\delta_{ij} + G_{ij}^a - \frac{\partial\langle U_i\rangle}{\partial x_j}. \tag{28}$$

It is well established[40] that linear stochastic equations such as Eq. (27) yield joint-normal processes. In particular, the one-time joint pdf of $\mathbf{u}^*$ is joint normal. Consequently, the pdf is completely determined by the means—which are zero—and by the covariance matrix

$$C_{ij}(t) \equiv \langle u_i^* u_j^*\rangle, \tag{29}$$

which is simply the Reynolds-stress tensor. From Eq. (27) it is readily deduced that C_{ij} evolves by

$$\dot{C}_{ij} = K_{il}C_{lj} + K_{jl}C_{li} + C_0\langle\epsilon\rangle\delta_{ij}. \tag{30}$$

In summary, for homogeneous turbulence, the generalized Langevin model results in a joint-normal one-time joint pdf of velocity ($\mathbf{u}^*$ or $\mathbf{u}$), with zero means, and covariances evolving according to Eq. (30).

For future use, we define $f(\mathbf{v},\zeta;t)$ to be the joint pdf of $\mathbf{u}^*$ and ϵ^*. That is, $f(\mathbf{v},\zeta;t)$ is the probability density of the joint event $[u_i^*(t) = v_i, \epsilon^*(t) = \zeta]$. Again, in homogeneous turbulence this is the same as the joint pdf of the Eulerian variables $\mathbf{u}$ and ϵ. For notational convenience we write the stochastic equation for ϵ^* as

$$d\epsilon^* = M(\epsilon^*)dt + D(\epsilon^*)dW, \tag{31}$$

where the drift $M(\epsilon^*)$ and diffusion $D(\epsilon^*)$ coefficients can be identified from Eq. (15). By standard techniques[11] the evolution equation for $f(\mathbf{v},\zeta;t)$ is obtained from the stochastic equations [Eqs. (27) and (31)]:

$$\frac{\partial f}{\partial t} = -K_{ij}\frac{\partial}{\partial v_i}(v_j f) + \frac{1}{2}C_0\langle\epsilon\rangle\frac{\partial^2 f}{\partial v_i\,\partial v_i} - \frac{\partial(MF)}{\partial\zeta} + \frac{1}{2}\frac{\partial^2(Df)}{\partial\zeta^2}. \tag{32}$$

Although we consider the joint pdf of $\mathbf{u}^*$ and ϵ^*, it should be noted that (according to the GLM) these processes are statistically independent. The coefficients (K_{ij} and $\langle\epsilon\rangle$) in the equation for $\mathbf{u}^*$ [Eq. (27)] are independent of ϵ^*; while those (M and D) in the equation for ϵ^* [Eq. (15)] are independent of $\mathbf{u}^*$.

B. Internal intermittency

One of the justifications for the Langevin model is that the predicted Lagrangian structure functions are in accord with the Kolmogorov (1941) hypotheses. The Lagrangian velocity structure function is defined by

$$D^{(L)}(s) \equiv \langle[\Delta_s U_1^+(t)]^2\rangle, \tag{33}$$

where the velocity increment is

$$\Delta_s U_1^+(t) \equiv U_1^+(t+s) - U_1^+(t), \tag{34}$$

(see Ref. 38, p. 359). For times s that are small compared to the integral time scale (τ, say) but large compared to the Kolmogorov scale τ_η, according to the Kolmogorov (1941) hypotheses the structure function is

$$D^{(L)}(s) = C_0\langle\epsilon\rangle s. \tag{35}$$

The Langevin equation [Eq. (22)] yields the same result for all times s much smaller than τ.

If internal intermittency is taken into account through the refined Kolomogrov (1962) hypotheses, Eq. (35) remains the prediction for the Lagrangian structure function. But a modification to the Langevin equation is called for. According to the model, Eq. (22), for small time intervals s ($s \ll \tau$), the velocity increment $\Delta_s U_1^*(t)$ is a Gaussian random variable with variance $C_0\langle\epsilon\rangle s$. This Gaussianity (with a constant variance) is clearly at odds with the notion of internal intermittency. In the spirit of Kolmogorov (1962) a better model would appear to be that $\Delta_s U_1^*(t)$ is a random variable with variance [conditional on the local dissipation $\epsilon^*(t)$] equal to $C_0\epsilon^*(t)s$. This, in turn, suggests that the diffusion coefficient $C_0\langle\epsilon\rangle$ in Eq. (22) be replaced by $C_0\epsilon^*$.

A generalization of the above suggestion has been investigated by Yeung and Pope[33] in their direct numerical simulations of statistically stationary homogeneous isotropic turbulence. It is found from the simulations that the flatness factor of $\Delta_s U_1^+(t)$ increases monotonically from the Gaussian value of 3 as s decreases. For very small s the flatness factor—essentially that of acceleration—is 11 and 18 in the simulations with $R_\lambda = 63$ and $R_\lambda = 90$, respectively. This is a clear indication of the non-Gaussian nature of $\Delta_s \mathbf{U}^+(t)$.

With the diffusion coefficient replaced by $C_0\epsilon^*$, the Langevin model implies that

$$q \equiv \Delta_s U_1^+(t)/\sqrt{\epsilon^+(t)}, \tag{36}$$

is Gaussian (for small s). From the simulations it is found that the flatness factor of q is 5.0 and 5.6 at the two Reynolds numbers. While these are in excess of the Gaussian value of 3, they represent a considerable reduction from 11 and 18.

It should be remembered that in Eq. (36), ϵ^+ is the pseudodissipation. If the true dissipation is used instead, the flatness factors obtained are 8.5 and 10.0. This is the second reason for using the pseudodissipation ϵ rather than the true dissipation ϵ_T—the first being that ϵ is more nearly lognormal.

C. Refined Langevin model

The model proposed here is (for homogeneous turbulence)

$$du_i^* = K_{ij}u_j^*\,dt + H_i\,dt + (C_0\epsilon^*)^{1/2}\,dW_i. \tag{37}$$

Compared to the GLM [Eq. (27)], an additional drift term $\mathbf{H}\,dt$ is introduced, and the diffusion coefficient is changed to $C_0\epsilon^*$ to account for internal intermittency, as argued above. For this reason we refer to Eq. (37) as the refined Langevin model (RLM). For small time intervals s, the diffusion term dominates, and yields:

$$\langle \Delta_s u_i^* \Delta_s u_j^* | \epsilon^* \rangle = C_0\epsilon^* s\delta_{ij}. \tag{38}$$

That is, the covariance of $\Delta_s \mathbf{u}^*$ conditional on the local dissipation ϵ^* is isotropic and proportional to ϵ^*. The isotropy of $\Delta_s \mathbf{u}^*$ (for small s) is consistent with Kolmogorov's hypothesis of local isotropy—as is also the case for the GLM.

The additional general drift term $\mathbf{H}(\mathbf{u}^*,\epsilon^*)$ in Eq. (37) is to be chosen so that the one-time joint pdf of $\mathbf{u}^*$ and ϵ^*, $f(\mathbf{v},\zeta;t)$, evolves in the same way as it does according to the GLM [Eq. (32)]. This is the appropriate requirement, since Eq. (32) yields the correct pdf evolution—$\mathbf{u}^*(t)$ is joint normal with the correct covariance matrix $C_{ij}(t)$.

The evolution equation for $f(\mathbf{v},\zeta;t)$ obtained from the refined model [Eq. (37)] is

$$\frac{\partial f}{\partial t} = -K_{ij}\frac{\partial(v_j f)}{\partial v_i} - \frac{\partial(fH_i(\mathbf{v},\zeta))}{\partial v_i} + \frac{1}{2}C_0\epsilon^*\frac{\partial^2 f}{\partial v_i\,\partial v_i} - \frac{\partial(Mf)}{\partial\zeta} + \frac{1}{2}\frac{\partial^2(Df)}{\partial\zeta^2}. \tag{39}$$

The difference between the right-hand sides of Eqs. (32) and (39) is

$$E(\mathbf{v},\zeta) \equiv -\frac{\partial(fH_i)}{\partial v_i} + \frac{1}{2}C_0(\epsilon^* - \langle\epsilon\rangle)\frac{\partial^2 f}{\partial v_i\,\partial v_i}, \tag{40}$$

and consequently the required choice of H_i is that which makes E vanish. By construction, the one-time joint pdf of $\mathbf{u}^*(t)$ is joint normal and independent of $\epsilon^*(t)$. Hence (as a property of the joint-normal distribution) we have

$$\frac{\partial f}{\partial v_i} = -C_{ij}^{-1}v_j f, \tag{41}$$

where C_{ij}^{-1} denotes the i-j component of the inverse of the Reynolds-stress tensor. Substituting this expression into Eq. (40) we obtain

$$E(\mathbf{v},\zeta) = \frac{\partial}{\partial v_i}\left(-fH_i - \frac{1}{2}C_0(\epsilon^* - \langle\epsilon\rangle)C_{ij}^{-1}v_j f\right). \tag{42}$$

Evidently, the required choice of $\mathbf{H}$ is

$$H_i = -\tfrac{1}{2}C_0(\epsilon^* - \langle\epsilon\rangle)C_{ij}^{-1}v_j. \tag{43}$$

There is advantage in reexpressing Eq. (43) by introducing the normalized Reynolds-stress tensor

$$A_{ij} \equiv 3C_{ij}/C_{ll} = \langle u_i u_j\rangle/(\tfrac{2}{3}k). \tag{44}$$

The trace A_{ii} is 3; and if the Reynolds stresses are isotropic, then $A_{ij} = A_{ij}^{-1} = \delta_{ij}$. With this definition, Eq. (43) becomes

$$H_i = -\tfrac{3}{4}C_0(\omega^* - \langle\omega\rangle)A_{ij}^{-1}v_j. \tag{45}$$

The refined Langevin model [Eq. (37)] is, then,

$$du_i^* = \left[K_{ij} - \tfrac{3}{4}C_0(\omega^* - \langle\omega\rangle)A_{ij}^{-1}\right]u_j^*\,dt + (C_0\epsilon^*)^{1/2}\,dW_i. \tag{46}$$

Or, in terms of the full velocity $\mathbf{U}^*(t)$ it is

$$dU_i^* = -\frac{1}{\rho}\frac{\partial\langle p\rangle\,dt}{\partial x_i} + L_{ij}(U_j^* - \langle U_j\rangle)dt + (C_0\epsilon^*)^{1/2}\,dW_i, \tag{47}$$

where

$$L_{ij} = G_{ij} - \tfrac{3}{4}C_0(\omega^* - \langle\omega\rangle)A_{ij}^{-1} = G_{ij}^a - (\tfrac{1}{2} + \tfrac{3}{4}C_0)\langle\omega\rangle\delta_{ij} - \tfrac{3}{4}C_0(\omega^* - \langle\omega\rangle)A_{ij}^{-1}. \tag{48}$$

These two equations [Eqs. (46) and (47)] can be compared to Eqs. (27) and (22) for the GLM. For isotropic turbulence without mean velocity gradients, the RLM adopts the simple form:

$$d\mathbf{u}^* = -(\tfrac{1}{2}\langle\omega\rangle + \tfrac{3}{4}C_0\omega^*)\mathbf{u}^*\,dt + (C_0\epsilon^*)^{1/2}\,d\mathbf{W}. \quad (49)$$

To summarize the properties of the refined Langevin model: For small time intervals s, the velocity increment $\Delta_s\mathbf{u}^*$ is isotropic with (conditional) variance proportional to $\epsilon^* s$. The one-time joint pdf of $\mathbf{u}^*$ and ϵ^* evolves identically to that corresponding to the GLM. In particular (at time t), $\mathbf{u}^*(t)$ is joint normal, and $\mathbf{u}^*(t)$ and $\epsilon^*(t)$ are independent. However, in contrast to the GLM, the multitime statistics of $\mathbf{u}^*$ are not joint normal, nor are they independent of ϵ^*.

Some variants of the refined Langevin model are discussed in Appendix B, where the question of realizability is also addressed.

IV. JOINT pdf EQUATIONS

Having obtained stochastic models for $\epsilon^*(t)$ [or, equivalently, for $\omega^*(t)$] and for $\mathbf{U}^*(t)$, in this section we write down the corresponding one-time joint pdf equations.

Let $F(\mathbf{V},\zeta;\mathbf{x},t)$ be the Eulerian one-point joint pdf of $\mathbf{U}$ and ϵ. The evolution equation for F can be derived by standard techniques[11] from the stochastic equations for $\mathbf{U}^*(t)$ [Eq. (47)] and $\epsilon^*(t)$ [Eq. (15)]:

$$\frac{\partial F}{\partial t} + V_i\frac{\partial F}{\partial x_i} = \frac{1}{\rho}\frac{\partial\langle p\rangle}{\partial x_i}\frac{\partial F}{\partial V_i} - L_{ij}\frac{\partial}{\partial V_i}\times(F[V_j - \langle U_j\rangle]) + \frac{1}{2}C_0\zeta\frac{\partial^2 F}{\partial V_i\,\partial V_i} + \langle\omega\rangle\frac{\partial}{\partial\zeta}\left(F\zeta\left\{S_\epsilon + C_\chi\left[\ln\left(\frac{\zeta}{\langle\epsilon\rangle}\right) - \frac{1}{2}\sigma^2\right]\right\}\right) + C_\chi\langle\omega\rangle\sigma^2\frac{\partial^2(F\zeta)}{\partial\zeta^2}. \quad (50)$$

Similarly, let $G(\mathbf{V},\theta;\mathbf{x},t)$ be the Eulerian one-point joint pdf of $\mathbf{U}$ and ω. Its evolution equation is

$$\frac{\partial G}{\partial t} + V_i\frac{\partial G}{\partial x_i} = \frac{1}{\rho}\frac{\partial\langle p\rangle}{\partial x_i}\frac{\partial G}{\partial V_i} - L_{ij}\frac{\partial}{\partial V_i}\times(G[V_j - \langle U_j\rangle]) + \frac{1}{2}C_0 k\theta\frac{\partial^2 G}{\partial V_i\,\partial V_i} + \langle\omega\rangle\frac{\partial}{\partial\theta}\left(G\theta\left\{S_\omega + C_\chi\left[\ln\left(\frac{\theta}{\langle\omega\rangle}\right) - \frac{1}{2}\sigma^2\right]\right\}\right) + C_\chi\langle\omega\rangle\sigma^2\frac{\partial^2(G\theta)}{\partial\theta^2}. \quad (51)$$

Starting from the Navier–Stokes equations, it is possible to derive exact evolution equations for F and G that can be compared to their modeled counterparts [Eqs. (50) and (51)]. For the joint pdf of velocities, this exercise has been performed by Haworth and Pope.[12] We do not perform the analogous exercise here because the exact equation of ϵ is uninformative: The dominant terms in the equation pertain to microscale processes, whereas the rate-controlling processes occur in the energy-containing range.

V. SPECIFICATION OF COEFFICIENTS

In this section, the coefficients in the model equations are specified. The emphasis of this work is on the form of the model and its qualitative performance. Consequently, simple specifications are made, sometimes by comparison to standard Reynolds-stress or pdf models. It is expected that modifications to these specifications in order to increase quantitative accuracy will be suggested by application of the model to a wide variety of inhomogeneous flows and also by a comparison to more recent modeling proposals (e.g., Refs. 8 and 9).

A. Dissipation equation

The stochastic model for $\epsilon^*(t)$ [Eq. (15)] contains three coefficients: σ^2, C_χ, and S_ϵ.

Values of σ^2—the variance of $\chi = \ln(\epsilon/\langle\epsilon\rangle)$—obtained from the direct numerical simulations of Yeung and Pope[33] are shown in Table I. It may be seen that (as expected) σ^2 increases weakly with Reynolds number: The DNS data suggest[33]

$$\sigma^2 = 0.29\ln R_\lambda - 0.36,$$

over the range investigated, $R_\lambda = 38$–93. However, rather than incorporating this dependence on R_λ, we choose instead to specify the constant value $\sigma^2 = 1.0$, corresponding to $R_\lambda \approx 110$. The reason for this decision is that the Reynolds-number dependence of other coefficients (e.g., C_χ and C_0) is not well established. To include Reynolds-number dependences in some coefficients and not in others is likely to lead to a spurious Reynolds-number dependence of the model as a whole. At present, the simpler strategy of making all coefficients independent of R_λ is likely to be more useful since, at high Reynolds numbers, very little Reynolds-number dependence is observed in one-point statistics (e.g., Reynolds stresses).

The constant C_χ is defined by [Eq. (10)]

$$C_\chi^{-1} = \langle\omega\rangle T_\chi = T_\chi/\tau, \quad (52)$$

where T_χ is the integral time scale of $\chi^+(t) \equiv \ln[\epsilon^+(t)/\langle\epsilon\rangle]$. Some care is needed in extracting the integral time scale T_χ from DNS, since artificial forcing is used to create statistically stationary turbulence. This, together with the periodic boundary conditions used, has a distorting effect on the energy containing motions—an effect which is patently displayed in the Eulerian energy spectrum. It appears, however, that the Lagrangian energy spectrum is little affected. Consequently, it can be expected that the ratio of T_χ to the Lagrangian velocity integral time scale T_u obtained from DNS is a reasonable estimate of the same quantity in natural turbulence. This time scale ratio T_χ/T_u is shown in Table I: On the basis of this data, C_χ is chosen to yield $T_\chi/T_u \approx 0.9$.

In Appendix A, the stochastic equations are analyzed, and an accurate (although approximate) expression for T_u/τ is obtained [Eq. (A45)]. This expression is used to deduce the value of C_χ that yields $T_\chi/T_u = 0.9$ for different values of C_0, for $\sigma^2 = 1$ (see Fig. 2). Thus, with $\sigma^2 = 1$, the specification $T_\chi/T_u = 0.9$ determines C_χ in terms of C_0. In the next subsection, the specification $C_0 = 3.5$ is made: the corresponding value of C_χ is (from Fig. 2) $C_\chi = 1.6$.

The normalized decay rate of $\langle\epsilon\rangle$, S_ϵ [Eq. (13)], or of $\langle\omega\rangle$, S_ω [Eq. (17)], is specified by Eq. (14) or Eq. (20), for consistency with the standard model equation for $\langle\epsilon\rangle$.

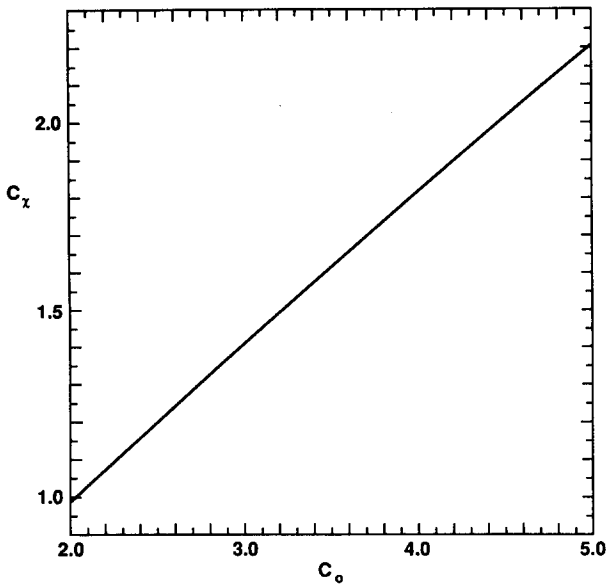

FIG. 2. The value of C_χ as a function of C_0 that yields $T/T_u = 0.9$ for $\sigma^2 = 1$ [from Eq. (A45)].

B. Specification of C_0

The choice of C_0 requires some discussion, since there is superficially conflicting evidence.

First, we recall that C_0 is a universal Kolmogorov constant.[10,38,41] We define the function $\widehat{C}_0(s)$ by

$$\widehat{C}_0(s) \equiv D^{(L)}(s)/(\langle\epsilon\rangle s), \tag{53}$$

where $D^{(L)}(s)$ is the second-order Lagrangian velocity structure function [Eq. (33)]. According to the Kolmogorov (1941 and 1962) hypotheses, at high Reynolds number, and for time intervals s in the inertial range ($\tau_\eta \ll s \ll \tau$), $\widehat{C}_0(s)$ adopts a constant value C_0. As mentioned in Sec. III, the stochastic models yield the same result for $s \ll \tau$.

Since Lagrangian statistics are extremely difficult to measure, there are no direct measurements of $\widehat{C}_0(s)$ at high Reynolds number. In their simulations, Yeung and Pope[33] find that $\widehat{C}_0(s)$ does not adopt a constant value over a range of s. (This observation does not conflict with the Kolmogorov hypotheses since the Reynolds numbers are insufficient for there to be a distinct inertial range.) The peak value of $\widehat{C}_0(s)$, denoted by C_0^*, appears to increase as $R_\lambda^{1/2}$, having the value 4.0 at the highest Reynolds number ($R_\lambda = 93$). These observations suggest that C_0 is larger than 4.0 (although there is no necessity for C_0^* to increase monotonically with R_λ).

Anand and Pope[18] deduced the significantly smaller value of $C_0 = 2.1$. They used the simplified Langevin model to make calculations of turbulent dispersion in grid turbulence. For this model and flow, C_0 is the only undetermined parameter and it is found that the value $C_0 = 2.1$ produces agreement with experimental data. With the refined Langevin model, however, turbulent dispersion is affected by σ^2 and C_χ in addition to C_0. Consequently, for the RLM, the effect of C_0 on dispersion is now reassessed.

The experiments[14–16] are performed in grid-generated turbulence. At a distance x_0 downstream of the grid, a fine heated wire is placed across the wind tunnel normal to the mean flow direction. At distances x' downstream of the wire, the profile of the mean excess temperature—which is Gaussian—is measured, and its standard deviation is denoted by σ'. Figure 3 shows σ'/l plotted against x'/x_0, where l is the value of $k^{3/2}/\langle\epsilon\rangle$ at the wire. In addition to the experimental data,[15] the figure shows the result given by the stochastic model with $C_0 = 2.0$, 3.5, and 5.0. In each case the value of C_χ is chosen to yield $T_\chi/T_u = 0.9$ (see Fig. 2) and σ^2 is unity. It may be seen that the data suggest a value of C_0 in the range 2–5, and that the sensitivity is small: increasing C_0 from 2 to 5 results in only 25% decrease in σ'/l.

It is clear that there remains considerable uncertainty in the value of C_0. Based on the observations made above, we tentatively specify the value $C_0 = 3.5$.

There is a direct correspondence between the simplified Langevin model (both standard and refined) and Rotta's return-to-isotropy model.[42] According to the simplified models (i.e., $G_{ij}^a = 0$), the Reynolds-stress tensor evolves (in homogeneous turbulence) according to [Eq. (30)]:

$$\frac{d}{dt}\langle u_i u_j\rangle = -\langle u_k u_j\rangle \frac{\partial\langle U_i\rangle}{\partial x_k} - \langle u_k u_i\rangle \frac{\partial\langle U_j\rangle}{\partial x_k} - \frac{2}{3}\langle\epsilon\rangle\delta_{ij} - \left(1 + \frac{3}{2}C_0\right)\langle\omega\rangle \times\left(\langle u_i u_j\rangle - \frac{2}{3}k\delta_{ij}\right). \tag{54}$$

This is exactly the same as Rotta's model, with $(1 + \frac{3}{2}C_0)$ being the Rotta constant C_R. The choice $C_0 = 3.5$ corresponds to $C_R = 5.25$ which is negligibly outside the range 4–5 suggested[7] to be appropriate (with $G_{ij}^a = 0$).

C. Adjustment of G_{ij}^a

Haworth and Pope[12,13] used the value $C_0 = 2.1$ in the GLM, while with the refined model the higher value of $C_0 = 3.5$ is appropriate (as shown in the preceding subsection). Consequently, the change in C_0 necessitates a com-

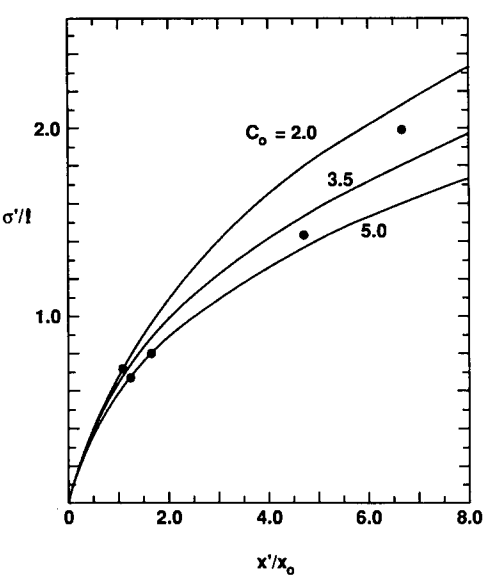

FIG. 3. Thermal wake width σ' against distance from the wire x'. Symbols, data of Warhaft;[15] lines RLM $C_0 = 2.0$, 3.5, 5.0.

pensating change in G_{ij}^a in order to yield the same (correct) evolution of Reynolds stresses in homogeneous turbulence. In this subsection the simple task of determining the required change in G_{ij}^a is performed.

Let the superscript a denote quantities used by Haworth and Pope:[13] in particular G_{ij}^a and $C_0^a = 2.1$. Let the superscript b denote the adjusted quantities, C_{ij}^b and $C_0^b = 3.5$ and let the differences be

$$\Delta C_0 \equiv C_0^b - C_0^a \tag{55}$$

and

$$\Delta G_{ij} \equiv G_{ij}^b - G_{ij}^a. \tag{56}$$

We require that the evolution of the Reynolds stresses [Eq. (30)] be the same for both models. Thus, from Eq. (30), we obtain

$$\Delta G_{ik} C_{kj} + \Delta G_{jk} C_{ki} + \Delta C_0 \langle \epsilon \rangle \delta_{ij} = 0. \tag{57}$$

It is possible, and helpful, to require ΔG_{ij} to be symmetric. Then, Eq. (57) uniquely determines ΔG_{ij} to be

$$\Delta G_{ij} = -\tfrac{1}{2} \Delta C_0 \langle \epsilon \rangle C_{ij}^{-1} = -\tfrac{3}{4} \Delta C_0 \langle \omega \rangle A_{ij}^{-1}. \tag{58}$$

In summary, the evolution of the Reynolds stresses is unaffected by a change in C_0, providing that G_{ij} is changed correspondingly according to Eq. (58).

VI. SUMMARY AND CONCLUSIONS

A modeled transport equation [Eq. (50)] has been obtained for the joint pdf of velocity and dissipation. This is achieved by constructing stochastic models for the velocity $\mathbf{U}^+(t)$ [Eq. (47)] and for the dissipation $\epsilon^+(t)$ [Eq. (15)] following fluid particles.

The pseudodissipation (rather than the true dissipation) is considered because of its favorable statistical properties. The logarithm of dissipation $\chi^+(t) \equiv \ln[\epsilon^+(t)/\langle \epsilon \rangle]$ is modeled by a Uhlenbeck–Ornstein process. Consequently, ϵ is lognormally distributed, and $\chi^+(t)$ has an exponential autocorrelation function, in accord with observations from direct numerical simulations.

The stochastic model for the Lagrangian velocity—the refined Langevin model—is a modification of the generalized Langevin model developed by Haworth and Pope.[12,13] The RLM accounts for internal intermittency, and in homogeneous turbulence yields the same, correct evolution of the joint pdf of velocity as the GLM. That is, the joint pdf of velocity is joint normal, with the Reynolds stresses evolving in accord with experimental observations.

The stochastic processes for $\mathbf{U}^*(t)$ and $\chi^*(t)$ are, or course, models and do not contain all of the physics embodied in the true time series $\mathbf{U}^+(t)$ and $\chi^+(t)$. For small times $s \ll \tau$, the autocorrelations of the (nondifferentiable) model processes decay linearly with s, while the true (differentiable) processes decay as s^2. For not-too-small times, the autocorrelation of $\chi^+(t)$ obtained from DNS (Fig. 1) appears approximately exponential—characterized by a single time scale—but at high Reynolds number a more complicated structure might be expected. For the velocity $\mathbf{U}^+(t)$, DNS again suggest an exponential autocorrelation: but it is possible that a more detailed examination for long time lags would reveal a power-law tail, indicative of long-term memory. [Molecular-dynamics studies[43] indicate $\rho_u(s) \sim s^{-3/2}$ for the autocorrelation of molecular velocities.]

In this paper attention is confined to homogeneous turbulence. And for this case *by construction* the model yields the correct evolution of the velocity-dissipation joint pdf. (Hence, a direct comparison with experimental data is not needed.)

The principal application of the modeled joint pdf equation is to inhomogeneous turbulent flows, both with and without chemical reactions. Applications to inhomogeneous flows are in progress.[32] An initial finding is that additional terms (that are zero for homogeneous turbulence) are required in the modeled joint pdf equation. Consequently, the equation developed here [Eq. (50)] should not be regarded as being directly applicable to inhomogeneous flows. Rather, the modeled equation for inhomogeneous flows (currently being developed) should reduce to Eq. (50) for the case of homogeneous turbulence.

For reacting flows, the appropriate joint pdf is that of velocity, dissipation, and composition.[2] The addition of composition to the velocity-dissipation pdf equation is straightforward. Furthermore, the inclusion of dissipation within the pdf provides the opportunity for improved modeling of mixing.

ACKNOWLEDGMENTS

We are grateful to Dr. M. S. Anand and Dr. D. C. Haworth for helpful comments on a draft of this paper.

This work is supported in part by contract "Combustion Design Model Evaluation" (F33615-87-C-2821) from the U. S. Air Force Wright Aeronautical Laboratories to Allison Gas Turbine Division, General Motors Corporation, and, in part, by the Grant No. CBT-8814655 from the National Science Foundation.

APPENDIX A: VELOCITY AND DISSIPATION AUTOCORRELATIONS

The primary purpose of this appendix is to obtain an expression for the Lagrangian velocity integral time scale. Several other useful results are obtained in the process.

1. One-time moments of dissipation

The normalized modeled dissipation is defined by

$$\gamma(t) \equiv \epsilon^*(t)/\langle \epsilon(t) \rangle. \tag{A1}$$

According to the model, $\gamma(t)$ is given by

$$\gamma(t) = \exp[\chi(t)], \tag{A2}$$

where $\chi(t)$ [denoted by $\chi^*(t)$ in the text] is a Uhlenbeck–Ornstein process with mean $-\frac{1}{2}\sigma^2$, variance σ^2, and integral time scale T_χ.

The general one-time mixed moment is defined by

$$M_{pq} \equiv \langle \gamma^p \chi^q \rangle, \tag{A3}$$

for $p > 0$, $q \geqslant 0$. By explicit integration over the pdf of χ we obtain

$$M_{pq} = \sigma^q \exp\left(\frac{1}{2}\sigma^2 p(p-1)\right)\frac{1}{\sqrt{2\pi}} \times \int_{-\infty}^{\infty} \left[z - \sigma\left(\frac{1}{2} - p\right)\right]^q \exp\left(-\frac{1}{2}z^2\right) dz. \quad \text{(A4)}$$

Hence (with $q = 0$), we obtain

$$\langle \gamma^p \rangle = \langle e^{p\chi} \rangle = \exp\left[\tfrac{1}{2}\sigma^2 p(p-1)\right]. \quad \text{(A5)}$$

With ξ being a standardized Gaussian random variable, it may be observed that Eq. (A4) is equivalent to

$$M_{pq} = \langle e^{p\chi} \rangle \sigma^q \langle \left[\xi - \sigma(\tfrac{1}{2} - p)\right]^q \rangle. \quad \text{(A6)}$$

Hence, in particular,

$$M_{p1} = \sigma^2(p - \tfrac{1}{2}) \exp\left[\tfrac{1}{2}\sigma^2 p(p-1)\right] \quad \text{(A7)}$$

and

$$M_{p2} = \sigma^2\left[1 + \sigma^2(p - \tfrac{1}{2})^2\right] \exp\left[\tfrac{1}{2}\sigma^2 p(p-1)\right]. \quad \text{(A8)}$$

2. Autocorrelation of dissipation

The UO process $\chi(t)$ is stationary, with autocorrelation function

$$\rho_\chi(s) = \exp(-s/T_\chi). \quad \text{(A9)}$$

The normalized dissipation $\gamma(t)$ is stationary with mean $M_{10} = 1$ and variance $(M_{20} - M_{10}^2) = \exp(\sigma^2) - 1$. The autocovariance and autocorrelation of γ are denoted by $R_\gamma(s)$ and $\rho_\gamma(s)$:

$$\rho_\gamma(s) = R_\gamma(s)/[\exp(\sigma^2) - 1]. \quad \text{(A10)}$$

The autocovariance is given by

$$R_\gamma(s) \equiv \langle [\gamma(t) - 1][\gamma(t+s) - 1] \rangle = \langle \exp(X) \rangle - 1, \quad \text{(A11)}$$

where

$$X \equiv \chi(t) + \chi(t+s). \quad \text{(A12)}$$

Now it is a property of the UO process[40] that $\chi(t)$ and $\chi(t+s)$ are jointly normal. Consequently, X is Gaussian; its mean and variance are

$$\langle X \rangle = \langle \chi(t) \rangle + \langle \chi(t+s) \rangle = -\sigma^2 \quad \text{(A13)}$$

and

$$\begin{aligned}\Sigma^2 &\equiv \operatorname{var}(X) \\ &= \langle \chi(t)^2 + 2\chi(t)\chi(t+s) + \chi(t+s)^2 \rangle - \langle X \rangle^2 \\ &= 2[\langle \chi^2 \rangle - \langle \chi \rangle^2] + 2\langle [\chi(t) - \langle \chi \rangle] \\ &\quad \times [\chi(t+s) - \langle \chi \rangle] \rangle \\ &= 2\sigma^2[1 + \rho_\chi(s)]. \end{aligned} \quad \text{(A14)}$$

Since X is Gaussian with known mean [Eq. (A13)] and variance [Eq. (A14)], $\langle \exp(X) \rangle$ and hence $R_\gamma(s)$ can be obtained by integrating over the pdf of X:

$$\begin{aligned} R_\gamma(s) &= \frac{1}{\Sigma\sqrt{2\pi}} \int_{-\infty}^{\infty} \exp\left(-\frac{(y + \sigma^2)^2}{2\Sigma^2}\right) e^y \, dy - 1 \\ &= \exp(\tfrac{1}{2}\Sigma^2 - \sigma^2) - 1 = \exp(\sigma^2 \rho_\chi[s]) - 1. \end{aligned} \quad \text{(A15)}$$

Hence, the autocorrelation of γ is

$$\begin{aligned} \rho_\gamma(s) &= [\exp(\sigma^2 \rho_\chi[s]) - 1][\exp(\sigma^2) - 1]^{-1} \\ &= \{\exp[\sigma^2 \exp(-s/T_\chi)] - 1\} \\ &\quad \times [\exp(\sigma^2) - 1]^{-1}. \end{aligned} \quad \text{(A16)}$$

The integral time scale of γ, T_γ, is obtained by

$$T_\gamma \equiv \int_0^\infty \rho_\gamma(s)\, ds = \int_0^\infty \frac{[\exp(\sigma^2 e^{-s/T_\chi}) - 1]\, ds}{(e^{\sigma^2} - 1)}. \quad \text{(A17)}$$

Substituting

$$y = \sigma^2 e^{-s/T_\chi}, \quad \text{(A18)}$$

we obtain

$$\begin{aligned} \frac{T_\gamma}{T_\chi} &= \int_0^{\sigma^2} \frac{(e^y - 1)}{y}\, dy \{e^{\sigma^2} - 1\}^{-1} \\ &= [\mathrm{Ei}(\sigma^2) - \ln \sigma^2 - \bar{\gamma}](e^{\sigma^2} - 1)^{-1} \\ &= \left(\sum_{n=1}^{\infty} \frac{\sigma^{2n}}{(nn!)}\right)\left(\sum_{n=1}^{\infty} \frac{\sigma^{2n}}{n!}\right)^{-1}, \end{aligned} \quad \text{(A19)}$$

where Ei is the exponential integral and $\bar{\gamma}$ is Euler's constant. It may be seen from the last expression that T_γ is less than T_χ. A plot of this ratio as a function of σ^2 is shown in Fig. 4. It may be seen that for σ^2 less than 2, say, Eq. (A19) is reasonably approximated by

$$T_\gamma/T_\chi \approx 1 - \tfrac{2}{5}\sigma^2. \quad \text{(A20)}$$

For $\sigma^2 = 1$, the autocorrelation $\rho_\gamma(s)$ [Eq. (A16)] is plotted in Fig. 5, and compared to the exponential

$$\rho_\gamma(s) \approx \exp(-s/T_\gamma), \quad \text{(A21)}$$

which, it may be seen, provides a good approximation.

3. Stochastic model for scaled velocity

For isotropic turbulence without mean velocity gradients, the refined stochastic model for velocity reduces to

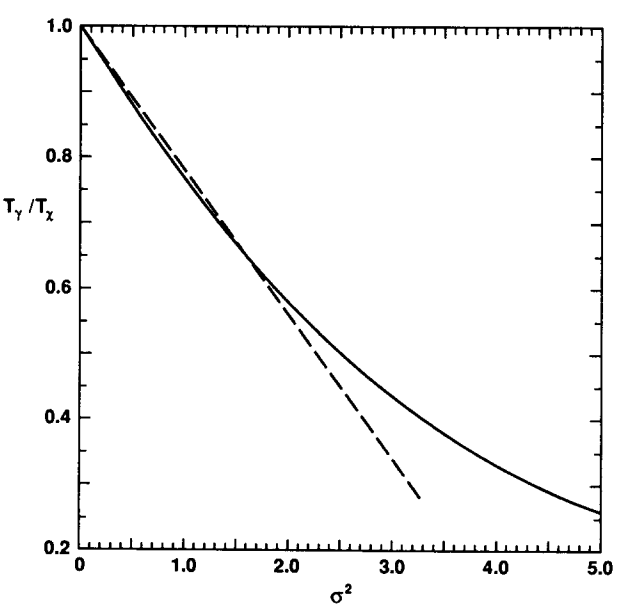

FIG. 4. Integral time scale ratio T_γ/T_χ against variance σ^2. The dashed line is the approximation Eq. (A20).

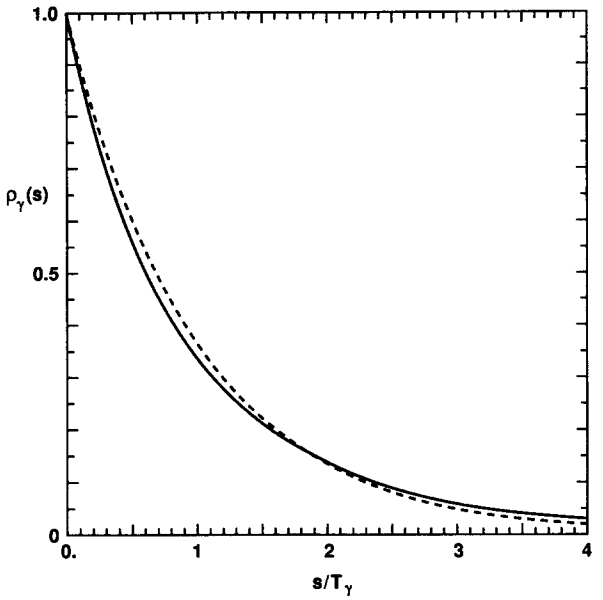

FIG. 5. Autocorrelation of γ. Solid line, Eq. (A16); dashed line, the approximation Eq. (A21).

$$d\mathbf{u}^* = -(\tfrac{1}{2}\langle\omega\rangle + \tfrac{3}{4}C_0\omega^*)\mathbf{u}^*\,dt + (C_0\epsilon^*)^{1/2}\,d\mathbf{W}. \tag{A22}$$

This process $\mathbf{u}^*(t)$ can be made stationary (even in decaying turbulence) by scaling all variables by $k(t)$ and $\langle\omega(t)\rangle$. Accordingly, we define $\hat{t}$ and $\hat{\mathbf{W}}$ by

$$d\hat{t} \equiv \langle\omega(t)\rangle dt \tag{A23}$$

and

$$d\hat{\mathbf{W}} \equiv \langle\omega(t)\rangle^{1/2}\,d\mathbf{W}, \tag{A24}$$

and the scaled velocity by

$$\hat{\mathbf{u}}(\hat{t}) \equiv \mathbf{u}^*(t)/k(t)^{1/2}. \tag{A25}$$

With these definitions, Eq. (A22) transforms to

$$d\hat{\mathbf{u}}(\hat{t}) \equiv \hat{\mathbf{u}}(\hat{t}+d\hat{t}) - \hat{\mathbf{u}}(\hat{t}) = -\tfrac{3}{4}C_0\gamma\hat{\mathbf{u}}\,d\hat{t} + (C_0\gamma)^{1/2}\,d\hat{\mathbf{W}}. \tag{A26}$$

It is readily shown that this stochastic differential equation yields a stationary process $\hat{\mathbf{u}}(t)$, with zero mean, and covariance $\frac{2}{3}\delta_{ij}$.

A further transformation is performed to yield a UO process in a stochastically scaled time. This time r is defined by

$$r(\hat{t}) \equiv \int_0^{\hat{t}} \gamma(\hat{t})\,d\hat{t}. \tag{A27}$$

The corresponding velocity and Wiener process are

$$\tilde{\mathbf{u}}(r[\hat{t}]) = \hat{\mathbf{u}}(\hat{t}) \tag{A28}$$

and

$$d\tilde{\mathbf{W}} = \gamma^{1/2}(\hat{t})\,d\hat{\mathbf{W}}. \tag{A29}$$

Corresponding to Eq. (A26), the stochastic differential equation for $\tilde{\mathbf{u}}(r)$ is

$$d\tilde{\mathbf{u}}(r) \equiv \tilde{\mathbf{u}}(r+dr) - \tilde{\mathbf{u}}(r) = -\tfrac{3}{4}C_0\tilde{\mathbf{u}}\,dr + C_0^{1/2}\,d\tilde{\mathbf{W}}. \tag{A30}$$

This corresponds to a UO process with mean zero, covariance $\frac{2}{3}\delta_{ij}$, and autocorrelation (in scaled time r)

$$\tilde{\rho}(s) = \exp(-s/\tilde{T}), \tag{A31}$$

where the (normalized) integral time scale is

$$\tilde{T} = (\tfrac{3}{4}C_0)^{-1}. \tag{A32}$$

This transformed equation [Eq. (A26)] is used below to obtain an expression for the velocity autocorrelation. But it also has an interesting interpretation. The Langevin equation (with diffusion coefficient $C_0\langle\epsilon\rangle$) yields a UO process (in regular time) for $\hat{\mathbf{u}}(\hat{t})$, with autocorrelation given by Eqs. (A31) and (A32). Accounting for internal intermittency (i.e., using $C_0\epsilon^*$ for the diffusion coefficient) yields exactly the same UO process, but in stochastically scaled time, r—scaled, that is, by the local dissipation rate $[dr = (\epsilon^*/\langle\epsilon\rangle)d\hat{t}]$.

4. Velocity autocorrelation

With some approximations, an expression is obtained for the autocorrelation $\rho_u(s)$ of one component of $\hat{\mathbf{u}}(\hat{t})$ given by Eq. (A26). Recalling that $\hat{u}_1(\hat{t})$ is stationary with variance $\frac{2}{3}$, the autocorrelation can be obtained from

$$\rho_u(s) = \tfrac{3}{2}\langle\hat{u}_1(0)\hat{u}_1(s)\rangle. \tag{A33}$$

In terms of the locally scaled UO process $\tilde{\mathbf{u}}(r)$ [Eq. (A30)], from Eqs. (A28), (A31), and (A33) we have

$$\rho_u(s) = \tfrac{3}{2}\langle\tilde{u}_1(0)\tilde{u}_1(r[s])\rangle = \langle\tilde{\rho}(r[s])\rangle = \langle\exp(-r[s]/\tilde{T})\rangle. \tag{A34}$$

Thus $\rho_u(s)$ can be determined if the pdf of $r(s)$ is known.

Since $\langle\gamma\rangle$ is unity, from Eq. (A27) we obtain

$$\langle r(s)\rangle = \int_0^s \langle\gamma(\hat{t})\rangle d\hat{t} = s, \tag{A35}$$

and also

$$\langle r(s)^2\rangle = \int_0^s\int_0^s \langle\gamma(\hat{t})\gamma(t')\rangle d\hat{t}\,dt' = \int_0^s\int_0^s 1 + \langle\gamma'(\hat{t})\gamma'(t')\rangle d\hat{t}\,dt' = \int_0^s\int_0^s 1 + \langle\gamma'^2\rangle\rho_\gamma(\hat{t}-t')d\hat{t}\,dt', \tag{A36}$$

where γ' is the fluctuation $\gamma' = \gamma - \langle\gamma\rangle$, and ρ_γ is the autocorrelation of γ. Thus the variance of $r(s)$ is

$$\langle r'(s)^2\rangle = \langle\gamma'^2\rangle\int_0^s\int_0^s \rho_\gamma(\hat{t}-t')d\hat{t}\,dt' = 2\langle\gamma'^2\rangle\int_0^s (s-\hat{t})\rho_\gamma(\hat{t})d\hat{t}. \tag{A37}$$

Although the autocorrelation ρ_γ is known [Eq. (A16)], in order to perform the integral in Eq. (A37) analytically, we use instead the exponential approximation, Eq. (A21). Then Eq. (A37) becomes

$$\langle r'(s)^2\rangle = 2\langle\gamma'^2\rangle T_\gamma^2[\exp(-s/T_\gamma) + s/T_\gamma - 1]. \tag{A38}$$

The second, and final, approximation is that $r(s)$ is log-normally distributed—as it certainly is for small s. Let

$$q(s) \equiv \ln[r(s)/\langle r(s)\rangle], \tag{A39}$$

have variance $\Sigma(s)^2$ and mean $-\frac{1}{2}\Sigma(s)^2$. From the relation

$$\langle e^{2q}\rangle = \langle r^2\rangle/\langle r\rangle^2, \tag{A40}$$

and Eq. (A38) we obtain

$$\Sigma(s)^2 = \ln\left[1 + 2\langle\gamma'^2\rangle(T_\gamma/s)^2(e^{-s/T_\gamma} + t/T_\gamma - 1)\right]. \tag{A41}$$

From Eqs. (A34), (35), and (39) we obtain

$$\rho_u(s) = \langle \exp(-se^q/\tilde{T})\rangle, \tag{A42}$$

and with the assumed Gaussianity of q:

$$\rho_u(s) = \frac{1}{\Sigma\sqrt{2\pi}}\int_{-\infty}^{\infty} \exp\left(-\frac{(\hat{q} + \frac{1}{2}\Sigma^2)^2}{2\Sigma^2} - \frac{s}{\tilde{T}}e^{\hat{q}}\right)d\hat{q}. \tag{A43}$$

With the transformation $y \equiv \frac{1}{2}\Sigma + \hat{q}/\Sigma$, the final expression is

$$\rho_u(s) = \frac{1}{\sqrt{2\pi}}\int_{-\infty}^{\infty} \exp\left\{-\frac{1}{2}y^2 - \frac{s}{\tilde{T}}\exp\left[\Sigma\left(y - \frac{1}{2}\Sigma\right)\right]\right\} dy. \tag{A44}$$

To summarize, with the assumptions that γ has an exponential autocorrelation function and that $r(s)$ is lognormally distributed, the autocorrelation of velocity is given by Eq. (A44). This expression can be evaluated numerically, and integrated (with respect to s) to give the Lagrangian velocity integral time scale:

$$T_u = \frac{1}{\langle\omega\rangle}\int_0^{\infty} \rho_u(s)\,ds. \tag{A45}$$

(In decaying turbulence both T_u and $\langle\omega\rangle$ depend upon time, but their product is constant.)

Since the expression for $\rho_u(s)$ [Eq. (A44)] is obtained via two approximations, some confirmation of its accuracy is called for. A Monte Carlo simulation was performed in which many sample paths of $\gamma(\hat{t})$ and $\hat{\mathbf{u}}(\hat{t})$ were generated numerically from their stochastic differential equations. Then $\rho_u(s)$ was determined using standard time-series analysis. Figure 6 shows $\rho_u(s)$ determined from the simulations compared to the approximate expression Eq. (A44). It may be seen that the agreement is excellent. (The conditions of the simulations are: $C_0 = 2.1$, $C_\chi = 2$, $\sigma^2 = 1$.)

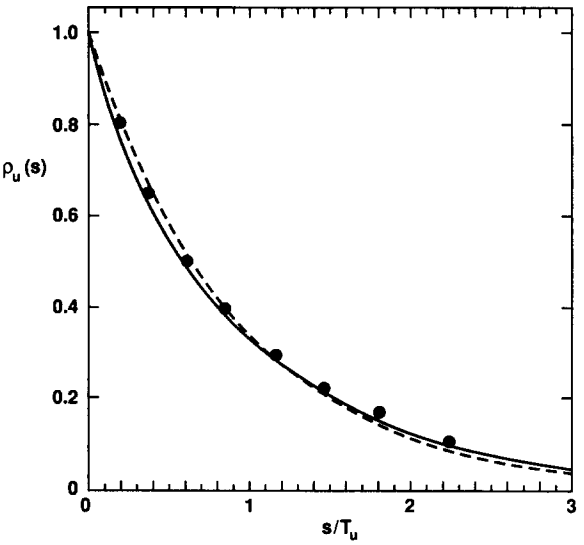

FIG. 6. Velocity autocorrelation. Solid line, Eq. (A44); dashed line, the approximation $\exp(-s/T_u)$; symbols, from Monte Carlo simulation ($C_0 = 2.1$, $C_\chi = 2$, $\sigma^2 = 1$).

APPENDIX B: VARIANTS OF THE REFINED LANGEVIN MODEL

The occurrence of the inverse of the Reynolds-stress tensor A_{ij}^{-1} in the refined Langevin model [Eqs. (46) and (47)] is a possible concern. Rapid rotation or stable stratification can cause turbulence to become two dimensional. As the two-dimensional state is approached, the Reynolds-stress tensor becomes singular, and hence some components of A_{ij}^{-1} tend to infinity. Thus, for flows that approach this two-dimensional limit, the occurrence of A_{ij}^{-1} is, at least, a possible source of ill conditioning. It appears, however, that the model does not violate realizability requirements, for the pdf evolution is identical for RLM and GLM, and it is known that GLM satisfies realizability.[11-13]

In the two subsections of this appendix two types of variants of the RLM are investigated, with a view to providing well-conditioned alternatives for turbulence close to the two-dimensional limit.

1. Approximate inverses

Three variants are described in which the inverse A_{ij}^{-1} appearing in the RLM [Eqs. (46)–(48)] is replaced by a different tensor $\tilde{A}_{ij}$. Then their performance is discussed.

a. Modified determinant (MD)

The inverse A_{ij}^{-1} can be written

$$A_{ij}^{-1} = A_{ij}^*/D, \tag{B1}$$

where D is the determinant of A_{ij}, and the tensor A_{ij}^* is finite even in the two-dimensional limit.

The determinant D is nondimensional and can take values between zero (for two-dimensional turbulence) and unity (for isotropic turbulence). In homogeneous shear flow its value is approximately 3/4.

We define the modified determinant $D^*(D)$ by

$$D^*(D) = D^2/(D + \gamma) + \gamma/(1 + \gamma), \tag{B2}$$

with $\gamma = 1/8$. This provides an excellent approximation to D—to within 1/2% for $D > 0.7$—and yet is positive for $D = 0$ [$D^*(0) = 1/9$].

The modified determinant (MD) model is defined by Eqs. (46)–(48) but with A_{ij}^{-1} replaced by

$$\tilde{A}_{ij} \equiv A_{ij}^*/D^* = A_{ij}^{-1}D/D^*. \tag{B3}$$

b. Approximate inverse (AI)

For application in different circumstances, it is useful to have a range of models—ranging from the most accurate available to the less accurate, but simpler. The GLM and simplified Langevin model (SLM) provide such a range. One aspect of the simplicity of the SLM is that it can be

implemented without the Reynolds stresses or mean velocity gradients being known (i.e., without their being extracted from the numerical solution of the joint pdf equation). However, this simplicity is partially removed in the refined Langevin model since it requires a knowledge of the Reynolds stress tensor (i.e., of A_{ij}^{-1}).

It is natural to examine, therefore, the simpler model (AI) defined by approximating A_{ij}^{-1} by the identity:

$$\widetilde{A}_{ij} \equiv \delta_{ij}. \tag{B4}$$

c. Neglect of inverse (NI)

Finally, for completeness, we define the NI model by

$$\widetilde{A}_{ij} = 0. \tag{B5}$$

An examination of the performance of this model demonstrates the importance of the term in $\widetilde{A}_{ij}$ in the RLM.

d. Performance of the models

For each model (RLM, MD, AI, NI) a Monte Carlo simulation was performed to determine the evolution of the joint pdf for the case of homogeneous shear flow. The conditions of the simulations are: $\partial \langle U_1 \rangle / \partial x_2 = 1$, $k(0) = 1$, $\langle \epsilon(0) \rangle = 0.3$ with $u_i(0)$ and $\ln \epsilon(0)$ having independent Gaussian distributions. The model constants used are $C_0 = 3.5$, $C_\chi = 1.6$, $G_{ij}^a = 0$, $\sigma^2 = 1.0$, $C_{\epsilon 1} = 1.45$, and $C_{\epsilon 2} = 1.9$.

Figure 7 shows the evolution of the flatness factor of $u_1(t)$, $F_u(t)$. The flatness factors for RLM and MD are indistinguishable, and equal to the Gaussian value of 3, to within the statistical error of the simulations. For AI, the flatness factor remains below 3.5, while for NI it exceeds 7.

For the evolution of the turbulent kinetic energy, Fig. 8, the conclusions are parallel: RLM and MD are indistinguishable, while AI deviates from these results less than NI.

From these results it can be concluded that the modified determinant model is well conditioned, and under normal

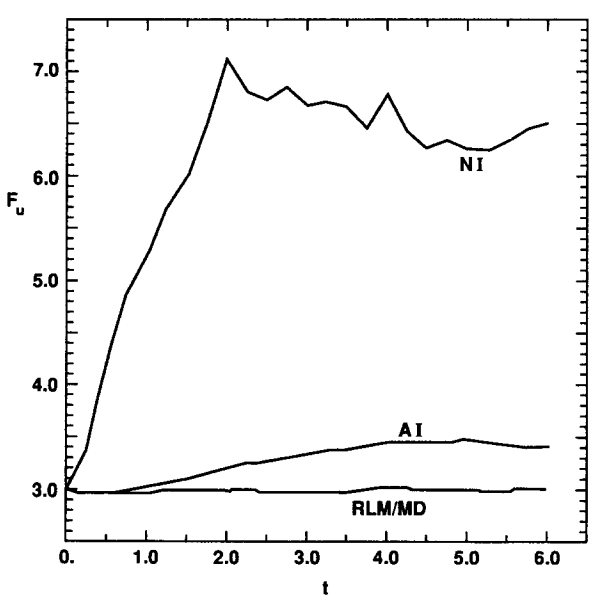

FIG. 7. Flatness factor of u_1 against time in homogeneous shear flow according to different models.

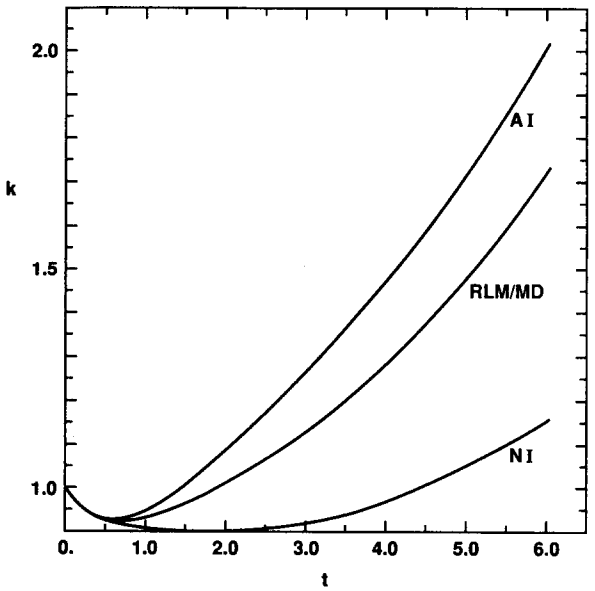

FIG. 8. Turbulent kinetic energy of u_1 against time in homogeneous shear flow according to different models.

circumstances (e.g., homogeneous shear) its performance is indistinguishable from RLM (and hence GLM). However, for two-dimensional turbulence non-Gaussian velocity pdf's occur. Approximating the inverse by the identity (AI) [Eq. (B4)] results in modest departures from Gaussianity. Thus AI is a reasonable approximate model, that can be implemented without the evaluation of the Reynolds-stress tensor.

2. Locally anisotropic model

The locally anisotropic model (LAM) is defined by

$$du_i^* = K_{ij}^A u_j^* \, dt + (C_0 \epsilon^*)^{1/2} A_{ij}^{1/2} \, dW_j, \tag{B6}$$

where K_{ij}^A is defined below, and $A_{ij}^{1/2}$ is the square root of A_{ij}, i.e., the symmetric tensor such that

$$A_{il}^{1/2} A_{lj}^{1/2} = A_{ij}. \tag{B7}$$

According to this model, for small time intervals s, the velocity increment is anisotropic: specifically

$$\langle \Delta_s u_i^* \, \Delta_s u_j^* | \epsilon^* \rangle = C_0 \epsilon^* s A_{ij}, \tag{B8}$$

[cf. Eq. (38)].

An analysis, similar to that performed in Sec. III C shows that the one-time joint pdf of $\mathbf{u}^*$ and ϵ^* evolves in the same way for this locally anisotropic model as it does for the refined Langevin model and for generalized Langevin models, provided that K_{ij}^A is specified to be

$$\begin{aligned} K_{ij}^A &= K_{ij} + \tfrac{3}{4} C_0 (\langle \omega \rangle A_{ij}^{-1} - \omega^* \delta_{ij}) \\ &= -(\tfrac{1}{2} \langle \omega \rangle + \tfrac{3}{4} C_0 \omega^*) \delta_{ij} + \tfrac{3}{4} C_0 \langle \omega \rangle (A_{ij}^{-1} - \delta_{ij}) \\ &\quad + G_{ij}^a - \frac{\partial \langle U_i \rangle}{\partial x_j}. \end{aligned} \tag{B9}$$

At first sight, this LAM provides no advantage over the RLM for two-dimensional turbulence, since it contains the inverse A_{ij}^{-1} in the definition of K_{ij}^A. However, the analysis shows that the joint pdf of velocity given by LAM is joint

normal providing only that the coefficient of ω^* is that given by Eq. (B9) (i.e., $\frac{3}{4}C_0\delta_{ij}$). If the coefficient $A_{ij}^{-1} - \delta_{ij}$ is replaced by an approximation $\widetilde{A}_{ij} - \delta_{ij}$ then the Reynolds-stress evolution is affected, but not the joint normality.

In summary, the locally anisotropic model is defined by Eqs. (B6) and (B9), with a finite approximation $\widetilde{A}_{ij}$ to A_{ij}^{-1}. Even for two-dimensional (homogeneous) turbulence this model yields a joint normal pdf of velocity. It is expected that a model applicable both to three-dimensional turbulence—in which local isotropy prevails—and to two-dimensional turbulence can be obtained by a blending of RLM and LAM.

[Simple analysis shows that the LAM is unaltered if, in Eq. (B6), the tensor $A_{ij}^{1/2}$ is replaced by any matrix Z_{ij} that satisfies $Z_{il}Z_{jl} = A_{ij}$. In the numerical implementation of the method it is convenient to make this replacement, taking Z_{ij} to be the Cholesky factorization[44] of A_{ij}.]

[1] *Whither Turbulence?* edited by J. L. Lumley (Springer, Berlin, in press).
[2] S. B. Pope in *23rd International Symposium on Combustion* (The Combustion Institute, Pittsburgh, in press).
[3] W. P. Jones and B. E. Launder, Int. J. Heat Mass Transfer **15**, 301 (1972).
[4] B. E. Launder and D. B. Spalding, *Mathematical Models of Turbulence* (Academic, New York, 1972).
[5] B. E. Lauder, G. J. Reece, and W. Rodi, J. Fluid Mech. **68**, 537 (1975).
[6] J. L. Lumley, J. Appl. Mech. **50**, 1097 (1983).
[7] B. E. Launder, in *Theoretical Approaches to Turbulence*, Applied Mathematical Sciences **58**, edited by D. L. Dwoyer, M. Y. Hussaini, and R. G. Voigt (Springer, Berlin, 1985).
[8] T. Craft, S. Fu, B. E. Launder, and D. P. Tselepidakis, University of Manchester Institute of Science and Technology, Mech. Eng. Rep. No. TFD/89/1 (1989).
[9] C. G. Speziale, S. Sarkar, and T. B. Gatski, ICASE Rep. No. 90-5, NASA Langley Research Center (1990).
[10] S. B. Pope, Phys. Fluids **24**, 588 (1981).
[11] S. B. Pope, Prog. Energy Combust. Sci. **11**, 119 (1985).
[12] D. C. Haworth and S. B. Pope, Phys. Fluids **29**, 387 (1986).
[13] D. C. Haworth and S. B. Pope, Phys. Fluids **30**, 1026 (1987).
[14] A. A. Townsend, Aust. J. Sci. Res. Ser. A **2**, 451 (1949).
[15] Z. Warhaft, J. Fluid Mech. **144**, 363 (1984).
[16] H. Stapountzis, B. L. Sawford, J. C. R. Hunt, and R. E. Britter, J. Fluid Mech. **165**, 401 (1986).
[17] J. W. Deardorff, Phys. Fluids **21**, 525 (1978).
[18] M. S. Anand and S. B. Pope, in *Turbulent Shear Flows 4*, edited by L. J. S. Bradbury, F. Durst, B. E. Launder, F. W. Schmidt, and J. H. Whitelaw (Springer, Berlin, 1985), p. 46.
[19] P. A. Libby, Prog. Energy Combust. Sci. **11**, 83 (1985).
[20] M. S. Anand and S. B. Pope, Combust. Flame **67**, 127 (1987).
[21] S. B. Pope, in *Turbulent Shear Flows 3*, edited by L. J. S. Bradbury, F. Durst, B. E. Launder, F. W. Schmidt, and J. H. Whitelaw (Springer, Berlin, 1982), p. 113.
[22] D. C. Haworth and S. B. Pope, J. Comput. Phys. **72**, 311 (1987).
[23] S. B. Pope and S. M. Correa, in *21st International Symposium on Combustion* (The Combustion Institute, Pittsburgh, 1988), p. 1341.
[24] D. C. Haworth, M. C. Drake, S. B. Pope, and R. J. Blint, *22nd International Symposium on Combustion* (The Combustion Institute, Pittsburgh, 1989), p. 1341.
[25] M. S. Anand, S. B. Pope, and H. C. Mongia, in *Turbulent Reactive Flows*, Lecture Notes in Engineering (Springer, Berlin, 1989), Vol. 40, p. 672.
[26] D. C. Haworth and S. H. El Tahry, in *7th Symposium on Turbulent Shear Flows* (Stanford University, Stanford, CA, 1989), p. 13.1.
[27] D. C. Haworth and S. H. El Tahry, General Motors Res. Lab. Rep. No. GMR-6844 (1989).
[28] M. S. Anand, S. B. Pope, and H. C. Mongia, in Ref. 26, p. 3.3.
[29] S. B. Pope and D. C. Haworth, in *Turbulent Shear Flows 5*, edited by F. Durst, B. E. Launder, F. W. Schmidt, and J. H. Whitelaw (Springer, Berlin, 1987), p. 44.
[30] S. Veeravalli and Z. Warhaft, J. Fluid Mech. **207**, 191 (1989).
[31] S. Karlin and H. M. Taylor, *A Second Course in Stochastic Processes* (Academic, New York, 1981).
[32] S. B. Pope, in *Twelfth Symposium on Turbulence* (University of Missouri—Rolla, Rolla, MO, 1990).
[33] P. K. Yeung and S. B. Pope, J. Fluid Mech. **207**, 531 (1989).
[34] A. N. Kolmogorov, Izv. Acad. Sci. USSR; Physics **6**, 56 (1942).
[35] D. C. Wilcox, AIAA J. **26**, 1311 (1988).
[36] A. N. Kolmogorov, J. Fluid Mech. **13**, 82 (1962).
[37] A. M. Obukhov, J. Fluid Mech. **13**, 77 (1962).
[38] A. S. Monin and A. M. Yaglom, *Statistical Fluid Mechanics: Mechanics of Turbulence* (MIT, Cambridge, MA, 1975), Vol. 2.
[39] S. Tavoularis and S. Corrsin, J. Fluid Mech. **104**, 311 (1981).
[40] L. Arnold, *Stochastic Differential Equations: Theory and Applications* (Wiley, New York, 1974).
[41] A. M. Obukhov, Adv. Geophys. **6**, 113 (1959).
[42] J. C. Rotta, Z. Phys. **129**, 547 (1951).
[43] B. J. Alder and T. E. Wainwright, Phys. Rev. A **1**, 18 (1970).
[44] E. Isaacson and H. B. Keller, *Analysis of Numerical Methods* (Wiley, New York, 1966).